Reports

Growth Mechanism of Sputtered Films of $YBa_2Cu_3O_7$ Studied by Scanning Tunneling Microscopy

MARILYN HAWLEY, IAN D. RAISTRICK,* JEROME G. BEERY, ROBERT J. HOULTON

The surface microstructures of *c*-axis–oriented films of $YBa_2Cu_3O_7$, deposited by off-axis magnetron sputtering on MgO and $SrTiO_3$ single crystal (100) substrates, have been investigated with scanning tunneling microscopy and atomic force microscopy. There is strong evidence that the films nucleate as islands and grow by adding material to the edge of a spirally rising step. This results in columnar grains, each of which contains a screw dislocation at its center. This microstructure may be of significance in determining superconducting properties such as critical current, and represents a significant difference between thin films (especially those grown in situ) and bulk materials.

As DEPOSITION METHODS FOR $YBa_2Cu_3O_7$ have improved, obvious granularity in thin films has been much reduced. This is true with respect to both the microscopic appearance of the films and their electrical behavior. Weak-link character is absent from high-quality films, and their critical currents are limited by flux motion. A number of important questions related to structure and microstructure, and their influence on superconducting properties, however, remain unresolved. Foremost among these is the unknown nature of the defects responsible for flux pinning in thin films. In this report we describe microstructural results obtained on sputtered films of $YBa_2Cu_3O_7$ using scanning tunneling microscopy (STM) and atomic force microscopy (AFM), probes which reveal detail at a higher resolution than is possible with a standard scanning electron microscope.

Several types of defects have been identified in films of $YBa_2Cu_3O_7$ by transmission electron microscopy (TEM), x-ray diffraction and ion-beam channeling, including stacking faults in the *ab* planes (*1–4*), lattice-mismatch edge dislocations (*3, 5, 6*), various types of twin boundaries, antiphase boundaries (*3–4*) and low- and high-angle grain boundaries (*4*, 7). There is, however, no general agreement as to the nature of the defects that are primarily responsible for the superior flux-pinning properties of epitaxial thin films, as compared with bulk or polycrystalline materials. Critical current and flux-flow resistance measurements in which the applied magnetic field and current direction are aligned with respect to the crystallographic axes (*8, 9*) have demonstrated a strong angular dependence of J_c when **B** is moved slightly out of the *ab* plane. This dependence suggests an intrinsic pinning mechanism in the layered superconductors, and evidence for flux pinning by (110) mirror twin boundaries was found (*8*). Roas *et al.* (*9*) investigated the angular dependence of J_c on **B**, as the field was rotated through the *c*-axis direction. They found a broad maximum at low fields (0.5 to 3 T) and high temperatures (>60 K). The pinning was actually stronger for $\mathbf{B}\|c$ than for **B** perpendicular to *c* in some **B**,*T* regimes. Hylton and Beasley (*10*) have made estimates of the density of defects necessary to pin flux lines and found it to be much greater than the density of extended defects (which include stacking faults, edge dislocations) observed by TEM. They therefore proposed the existence of a large concentration of point defects such as oxygen vacancies which can presumably be relatively easily accommodated because of variable copper valence.

Other important aspects of the films which are not well understood are the mechanisms of nucleation and growth, how these are affected by substrate properties, and how they relate to grain structure and to the degree of alignment of the crystal lattice with the underlying substrate. Recent TEM studies of laser-ablated films of $YBa_2Cu_3O_7$ on MgO substrates (*11*) seem to show that island (rather than layer by layer) growth takes place, and that steps in the substrate surface are favorable nucleation sites. Pretreatments that favor steps (a high-temperature anneal, for example) apparently lead to improved epitaxial order and better superconducting properties (*12*).

We have deposited films of $YBa_2Cu_3O_7$ on MgO and $SrTiO_3$ (100)-oriented substrates by off-axis radio-frequency (RF) magnetron sputtering (*13*) at 100 mtorr total pressure (60:40 oxygen:argon), and an RF power of 50 W. Films on MgO were deposited at 705°C and the films on $SrTiO_3$ at 740°C. At the end of the deposition the chamber was flooded with pure oxygen to a pressure close to 1 atm and the films were cooled at a rate of about 10° per minute to 425°C, where they were maintained for 30 min. The films were approximately 200 nm thick, and were grown at a rate of 1 to 1.5 nm/min. Both substrates were obtained from Enprotech Inc. (*14*). The MgO was used without further pretreatment, but the $SrTiO_3$ was heated in air at 950°C for 30 min prior to the deposition.

X-ray diffraction indicated that the films were completely oriented with their *c*-axes perpendicular to the substrate, and had good in-plane epitaxy (<1% volume fraction misaligned). Ion-beam channeling experiments indicated that the material was of relatively high crystal quality, with (001) channeling yields usually close to, or less than, 10% (measured for the barium edge, behind the surface peak). This figure is significantly higher than that expected for perfect single crystals, and it is noticeable, especially in the films on MgO, that channeling is less good deeper into the films. This has been taken as evidence of mismatch dislocations, which are found close to the interface (*6*).

The superconducting transitions in these sputtered films occur at slightly reduced temperatures (85 to 87 K), when compared with bulk materials or post-annealed films (>90 K). Transitions were examined using both direct current and low frequency (10 kHz) eddy current methods and were very sharp in both cases. The somewhat low transition temperature (T_c) appears to be associated with an elongated *c*-axis lattice parameter, a correlation that has been noted by others (*13*) but is not well explained. The films have high transport critical-current densities ($J_c > 10^7$ A cm^{-2} at 64 K in zero field, $> 10^5$ A cm^{-2} at 6 T, $\mathbf{B}\|c$). We have imaged the free surfaces of films on both MgO and $SrTiO_3$ substrates using the Nanoscope II STM and AFM. The STM images were acquired in constant current mode with a cold-worked PtIr scanning tip. Sample bias voltages were typically 400 to 500 mV and set-point currents ranged from 100 to 300 pA. Either no filtering, or simple low-pass filtering to remove high-frequency noise, was employed in producing the final images. The AFM images were taken for the same samples, using a commercial Au-coat-

Los Alamos National Laboratory, Los Alamos, NM 87545.

*To whom correspondence should be addressed.

ed 100-μm triangular Si_3N_4 cantilever (force constant approximately 0.6 N m^{-1}). No special surface preparation of the films was necessary. The films were stored in a desiccator and, in general, were examined in the microscope within a few days of preparation. The low deposition rates appear to lead to well-equilibrated, and hence more stable, surfaces: a factor which may well contribute to the high quality of the images. The most striking features of the STM images, common to films prepared on both substrates (Fig. 1, A and B, MgO; Fig. 2, A and B, $SrTiO_3$), are the obvious granularity of the films and the spiral growth pattern of each grain.

The grain sizes are somewhat different for the two cases. On MgO the grain diameters are between 100 and 500 nm, and a clear anisotropy is evident: the grains have an elliptical or rectangular shape. On $SrTiO_3$ the largest grains are significantly bigger (often >1.0 μm), although small grains are also present (Fig. 2A), and have a more circular cross section. These differences may well be caused by the somewhat different deposition temperatures used for the two substrates.

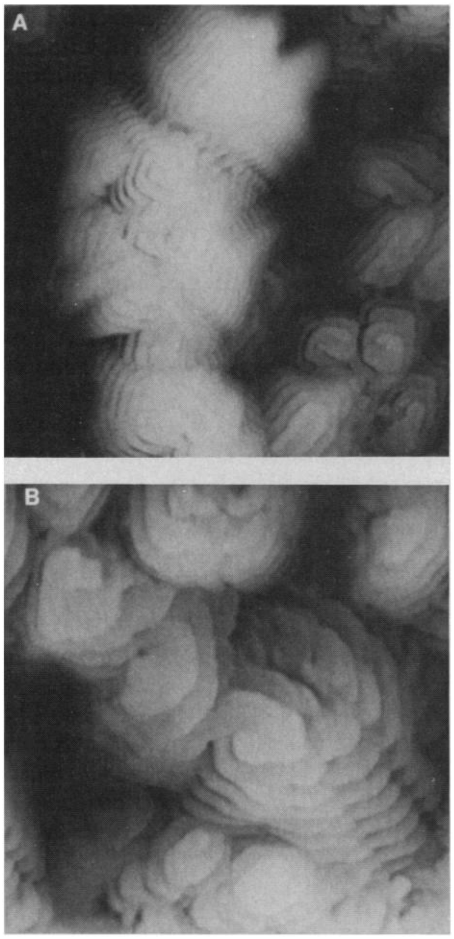

Fig. 1. (**A**) Low magnification STM image of a film deposited on MgO. The terraced surface and spiral growth pattern are clearly visible. The apparent "heights" of the various features are greatly exaggerated compared to the horizontal distances. The vertical height difference between terraces is one unit cell (1.17 nm) (image size: 1000 by 1000 nm). (**B**) Higher magnification image of a few grains of a film deposited on MgO (image size: 650 by 650 nm).

There is apparently another difference in the growth habit on the two substrates visible in the STM images. The terraces on the films deposited on MgO appear to be much flatter than those found in the films deposited on $SrTiO_3$, where each step edge seems to be separated from the one above or below by a sharp minimum.

As is true in any STM experiment, the exact interplay of electronic and topographical contributions to the surface structure seen in the image cannot be separated. With the addition, however, of the AFM capability, commonalities in the images observed with the two techniques can be confidently ascribed to topography. AFM imaging techniques duplicated faithfully most of the details of the grain structure produced by the STM (Fig. 3). In particular, the spiral growth pattern, overall grain sizes, and step-to-step horizontal and vertical distances within a grain were reproduced.

Of particular interest is the spiral growth pattern of the grains. The vertical height difference between "terraces" is often one unit cell, about 1.2 nm, although there also seems to be evidence for half and doubled *c*-axis periodicities in some grains. AFM and STM line scans across similar grains are shown in Fig. 4. In the AFM scans (Fig. 4, A and C) a sequence of steps and terraces is clearly seen. Each is approximately one unit cell deep. In the STM line scans a sharp dip often appears before the rise at each step. This effect is particularly noticeable in the scans of films prepared on $SrTiO_3$, (Fig. 4D), and it accounts for the different appearance of the terraces in the STM images mentioned above (for example, Fig. 2). The origin of this detail is unexplained at present. It is, however, reproducible over many scans, and over the entire surface of the film.

The implication of these observations is that each grain or column grows by adding atoms to a spirally expanding step on the top surface of the grain. Film growth, therefore, proceeds by an "island" growth mechanism rather than by the addition of new layers to a completed surface. This is exactly the classical spiral growth mechanism proposed by Frank (*15*) and developed theoretically by Burton, Cabrera, and Frank (*16*) for crystals grown under conditions of low supersaturation. This observation is consistent with the findings of the Cornell group who studied the early stages of film growth using TEM (*11*). In support of this growth model, we have also obtained preliminary results on a very thin film of $YBa_2Cu_3O_7$ on MgO (approximately 20 nm thick) using AFM and found exactly the same microstructure.

An important consequence of this growth pattern is that each grain incorporates a

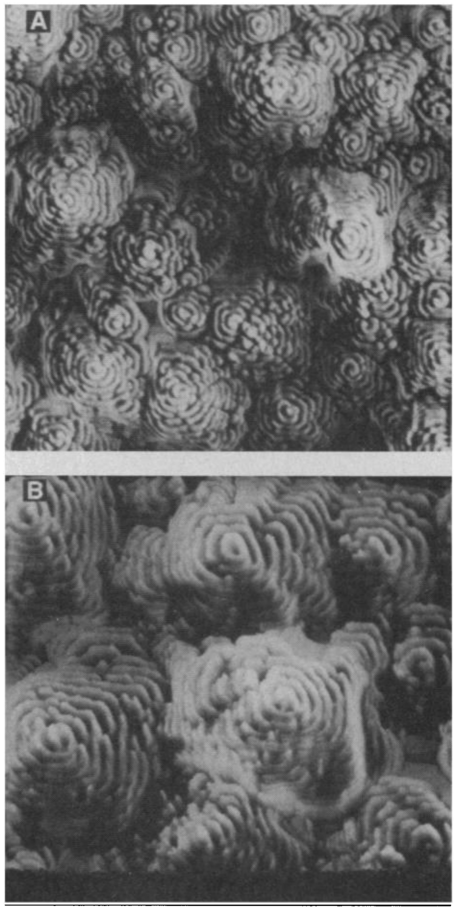

Fig. 2. (**A**) Low magnification STM image of a film deposited on $SrTiO_3$. Note that the horizontal scales and grain sizes are significantly different from those in Fig. 1 (image size 3700 by 3700 nm). (**B**) STM image of a few grains in a film on the $SrTiO_3$ substrate (image size 2070 by 2070 nm).

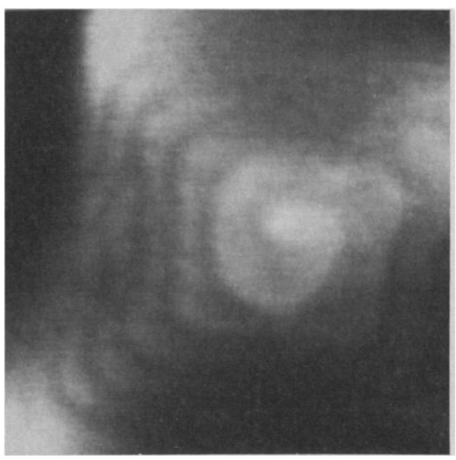

Fig. 3. AFM image of a single grain of a film grown on MgO (image size 157 by 157 nm).

screw dislocation that extends from the substrate interface all the way to the free film surface. This microstructure and its associated defects may have significant implications for the superconducting properties of the thin films themselves.

There are two types of defects which are present as a consequence of the growth. The first of these is the screw dislocation itself, which consists of a cylindrically symmetric stress field and a highly distorted core, and the second is the large number of sub-grain boundaries which arise as the neighboring growth islands impinge on one another.

A line defect, such as a screw dislocation, with a diameter comparable to the coherence length, that extends through the entire thickness of the film, probably represents an attractive pinning center for **B**$\|$*c* because it allows the flux line to be pinned along its entire length. The vortex may interact directly with a change in the order parameter in the core of the dislocation, brought about by disruption or distortion of the crystal structure of the superconductor, or with the stress field associated with the dislocation. For a screw, the strain is pure shear, and the effectiveness of the pinning depends on the difference between the shear modulus in the superconducting state and that in the normal state (*17, 18*). For a screw dislocation the quadratic coupling may be quite strong, especially when the flux line lies in the same direction as the dislocation vector. The dislocation will pin less effectively when it is perpendicular to the flux line.

The principal objection to the importance of the screw dislocations themselves as effective pinning centers is that there are relatively few of them, compared with the vortex density at high fields in the mixed state. For the case of the 200-nm-thick films on MgO, we may estimate from Fig. 1 a lower limit on the dislocation spacing (and hence, presumably, on the vortex spacing) of about 100 nm. This would effectively pin a macroscopic field of a few tenths of a tesla. Experimentally, however, we find that these films have excellent critical currents out to fields of at least 8 T (**B**$\|$*c*). Any contribution of the screw dislocations to pinning would appear, therefore, to be restricted to low fields.

Alternative flux-pinning sites in these films lie at the sub-grain boundaries and at the many defects that must be associated with them. Although coupling between the grains is excellent, as is shown by the high J_c's and absence of weak link behavior, the films are clearly not single crystal in nature.

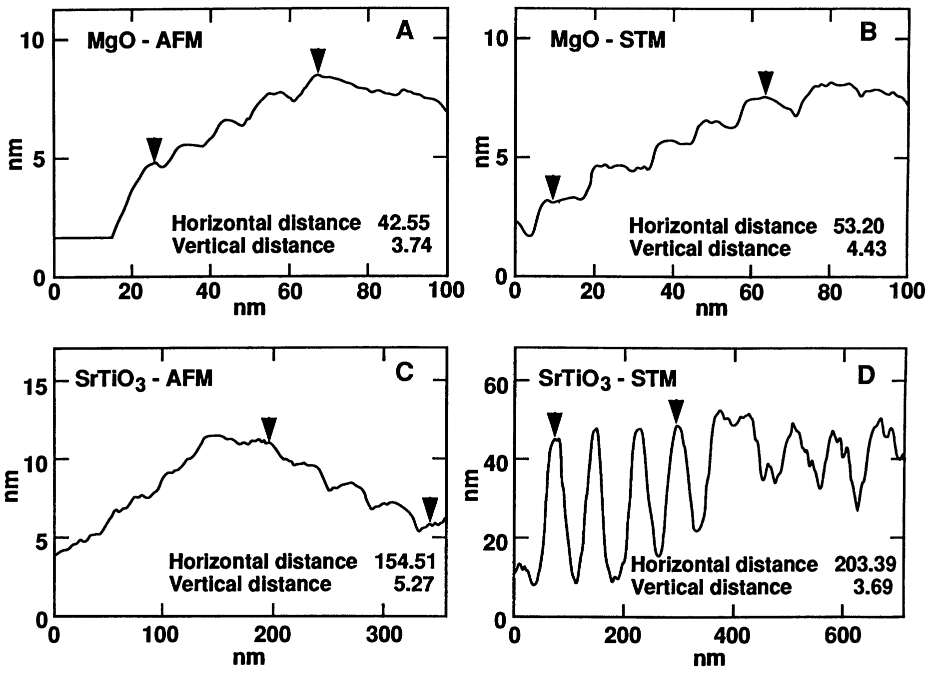

Fig. 4. STM and AFM line scans across individual grains. Distances between markers are given in nanometers.

There are many opportunities for mistakes in the orientation of the unit cells, as is evident from the figures presented here. This would result in many low-angle grain boundaries which are likely to contain edge dislocations and strain. Shin *et al.* (7) have identified certain defects that they believe are a consequence of island growth. Because of the growth mechanism, the grain boundaries form cells with approximately circular or polygonal cross sections, that extend through all or a considerable fraction of the film thickness. Each grain or cell wall could interact with many flux lines.

Although we have only demonstrated the presence of such defects in films grown under the particular conditions described above, it seems likely that the spiral columnar growth mechanism will be relatively general for films grown directly with the $YBa_2Cu_3O_7$ structure at low effective supersaturations. Because of the layered structure, the rapid growth direction of the films is in directions perpendicular to the *c*-axis, that is, material is most easily added at an edge. The spiral growth mechanism allows this process to be continued indefinitely, given well-controlled and stable growth conditions. The alternative growth mechanism, layer by layer growth, in which a new layer is nucleated on top of a completed, smooth surface will be very improbable in a four-component compound with a very anisotropic and atomistically inhomogeneous unit cell. At higher temperatures and effective supersaturations, a transition to a nucleation mechanism, leading to rough surfaces is a possibility.

REFERENCES AND NOTES

1. A. F. Marshall *et al.*, *Phys. Rev. B* **37**, 9353 (1988).
2. H. W. Zandbergen, R. Gronsky, G. Thomas, *Phys. Stat. Sol. (a)* **105**, 207 (1988).
3. R. Ramesh *et al.*, *Science* **247**, 57 (1990).
4. R. Ramesh *et al.*, *J. Mater. Res.* **5**, 704 (1990).
5. J. Chang *et al. Appl. Phys. Lett.* **54**, 2349 (1989).
6. J. Geerk, G. Linker, O. Meyer, *Mater. Sci. Rep.* **4**, 193 (1989).
7. D. H. Shin *et al.*, *Proceedings of the 47th Annual Meeting of the Electron Microscopy Society of America*, G. W. Bailey, Ed. (San Francisco Press, San Francisco, 1989), p. 174.
8. Y. Iye *et al.*, *Physica C* 166, 62 (1990).
9. B. Roas, L. Schultz, G. Saemann-Ischenko, *Phys. Rev. Lett.* **64**, 479 (1990).
10. T. L. Hylton and M. R. Beasley, *Phys. Rev. B* **41**, 11669 (1990).
11. M. G. Norton, L. A. Tietz, S. R. Sommerfelt, C. B. Carter, *Appl. Phys. Lett.* **55**, 2348 (1989).
12. B. H. Moeckley *et al.*, *ibid.* **57**, 1687 (1990).
13. C. B. Eom *et al.*, *ibid.* **55**, 595 (1989).
14. Enprotech Corp., 1 Station Square, Suite 620, Pittsburgh, PA 15219.
15. F. C. Frank, *Disc. Farad. Soc.* **5**, 48 (1949).
16. W. K. Burton, N. Cabrera, F. C. Frank, *Phil. Trans. Roy. Soc.* **A243**, 299 (1951).
17. H. Ullmaier, *Irreversible Properties of Type II Superconductors*, Springer Tracts in Modern Physics, No. 76 (Springer-Verlag, Berlin, 1975), p. 46.
18. A. M. Campbell and J. E. Evetts, *Adv. Phys.* **21**, 199 (1972).
19. We gratefully acknowledge the assistance of the following Los Alamos personnel: J. Martin and R. Dye for eddy current measurements; A. D. Rollett and T. Schofield for texture analysis; and F. H. Garzon, M. Maley, T. E. Mitchell, L. Campbell and P. Kes for valuable discussions.

27 December 1990; accepted 1 March 1991